



## A supramolecular host–guest complex for heparin binding and sensing†

Cite this: *Nanoscale*, 2018, **10**, 14022

Salla Välimäki,<sup>a</sup> Ngong Kodiah Beyeh,<sup>b,c,d</sup> Veikko Linko,<sup>b</sup> Robin H. A. Ras<sup>a,b,e</sup> and Mauri A. Kostiainen<sup>b,\*a,e</sup>

Heparin is an anionic polysaccharide widely used in clinics as an anticoagulant. However, heparin usage requires an antidote and sensors for safe operation during and after surgeries. In this study, a host–guest complex capable of selective heparin binding and sensing is presented. Heparin binding affinity was studied in solution with a variety of polycationic macrocyclic hosts, a pillar[5]arene and multiple resorcin[4]arenes, by dynamic light scattering, dye displacement assay, isothermal titration calorimetry, and anti-Xa assay. The measurements reveal the significant importance of multivalency in electrostatic host–heparin binding in competitive, application-relevant media. Additionally, to monitor the heparin concentration, a host–guest indicator displacement assay was performed by following the free and bound state of the methyl orange dye in UV-Vis spectroscopic experiments. Furthermore, this colorimetric sensing based on the tertiary host–guest–heparin supramolecular assembly was utilized in the construction of a calibration curve in a range of blood plasma concentrations.

Received 17th April 2018,  
Accepted 24th June 2018  
DOI: 10.1039/c8nr03132k  
rsc.li/nanoscale

### Introduction

Heparin is a naturally occurring highly charged polyanion and a well-known anticoagulant widely used in surgical practice.<sup>1</sup> More specifically, it is a negatively charged sulfated polysaccharide belonging to the group of glycosaminoglycans (Scheme 1). The anticoagulant effect of heparin is based on its ability to activate antithrombin-III, which, subsequently, inactivates vital coagulation cascade substances such as thrombin and factor Xa consequently preventing fibrin and clot formation.<sup>2</sup> To balance and neutralize heparin dosing, a heparin inhibitor is needed, and commonly, arginine-rich protein protamine sulfate (PS) is used for this purpose.<sup>3,4</sup> However, in recent years, there has been interest to investigate alternatives for protamine due to its adverse effects like hypotension and serious allergic reactions.<sup>5–7</sup> In the neutralization process, electrostatic interactions play a key role as the heparin–protamine

complex is formed due to the attractive forces arising from heparin's negative and protamine's positive charge. In addition to neutralization methods, sensing applications during and after surgery are also required for heparin concentration determination.<sup>3</sup> Commonly, the activated partial thromboplastin time (aPTT) technique and the anti-Xa assay are used.<sup>8</sup> However, these currently available analysis methods have certain limitations including preanalytical and postanalytical variabilities<sup>8,9</sup> leading to the need of improved heparin sensing systems.

Many colorimetric<sup>10–14</sup> and fluorescent<sup>15–30</sup> heparin sensors with different functionalities and varying structures from small molecules<sup>11,14,18–22</sup> and host–guest complexes<sup>16,24</sup> to synthetic polymers<sup>12,27–29</sup> and peptides<sup>31,32</sup> have been developed. For instance, a boronic acid based receptor utilizing the preorganization of the structure provided a colorimetric heparin indication system capable of selective heparin binding.<sup>11</sup> Amine and guanidine functional groups, on the other hand, were exploited in the development of self-assembling fluorescent receptors designed for electrostatic heparin binding.<sup>24</sup> In this system, a variety of cyclodextrin hosts and fluorescent guests were used to detect the purity of heparin. Additionally, induced fit of cationic calix[8]arenes has been used for heparin binding with improved complexation when compared to protamine.<sup>16</sup> This system also provides signaling that is based on indicator displacement monitored by fluorescence spectroscopy.

Inspired by these macrocyclic heparin sensors, we have designed a series of cationic macrocycles capable of heparin

<sup>a</sup>Department of Bioproducts and Biosystems, Aalto University, P.O. Box 16100, FI-00076 Aalto, Espoo, Finland

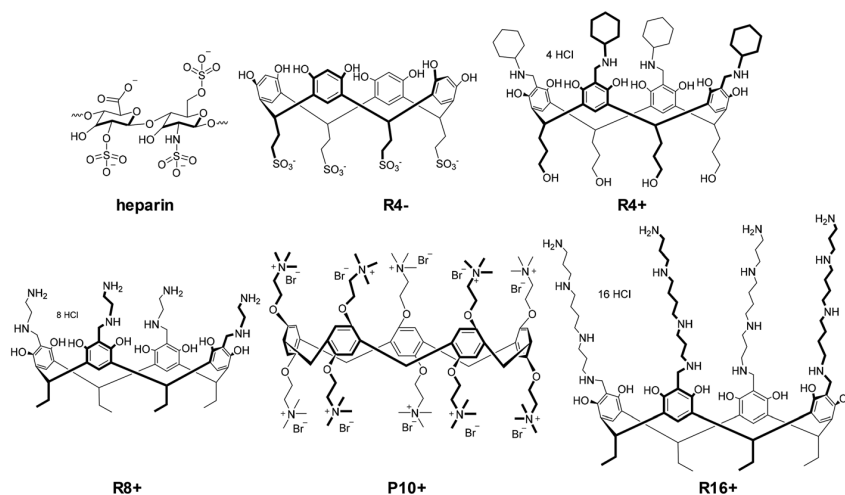
<sup>b</sup>Department of Applied Physics, Aalto University, P.O. Box 15100, FI-00076 Aalto, Espoo, Finland

<sup>c</sup>Department of Chemistry and Biochemistry, University of Windsor, Windsor, ON N9B 3P4, Canada

<sup>d</sup>Department of Chemistry, Oakland University, 146 Library Drive, Rochester, Michigan 48309-4479, USA

<sup>e</sup>HYBER Centre of Excellence, Department of Applied Physics, Aalto University, FI-00076 Aalto, Finland

†Electronic supplementary information (ESI) available. See DOI: 10.1039/c8nr03132k



**Scheme 1** Structure of the major repeating unit of heparin and macrocyclic hosts used in the study. Hosts are named based on their structure (P = pillar[5]arene, R = resorcin[4]arene) and a nominal number of charges.

binding in addition to host–guest binding. In more detail, we have studied resorcin[4]arenes and a pillar[5]arene with a varying number of positive charges and different cavity sizes (Scheme 1). Resorcinarenes, obtained from an acid catalyzed condensation between resorcinol and aldehydes, are well-known macrocyclic host systems for a wide variety of guests.<sup>33</sup> Pillararenes, on the other hand, are synthesized by linking hydroquinone ethers with methylene bridges to form rigid rings.<sup>34</sup> Both these macrocyclic receptors can be modified by attaching different functional groups on the lower and upper rims, and therefore these receptors have been developed for many applications, for example, in the areas of biomedicine<sup>35,36</sup> and materials science.<sup>34,37</sup> The resorcin[4]arenes used here exist in their  $C_{4v}$  crown conformation which is locked by intramolecular hydrogen bonds between adjacent hydroxyl groups at the upper rim. Further functionalization of the upper rim with amine containing moieties in a Mannich<sup>38,39</sup> condensation reaction with excess formaldehyde and subsequent ring opening with mineral acids<sup>40</sup> give the resorcin[4]arenes a cationic character that enables binding with anionic heparin. The pillar[5]arene used in this study has a characteristic pillar-like structure and cationic moieties on both upper and lower rims in addition to an electron-rich internal cavity accessible from both sides.<sup>41</sup> By increasing the number of charges in the host structures from +4 to +16, enhanced heparin binding is expected due to multivalency. An anionic resorcin[4]arene not expected to interact with heparin was included in the research as a control compound.<sup>42</sup>

Binding affinity between heparin and the resorcin[4]arenes (**R4-**, **R4+**, **R8+** and **R16+**) as well as the pillar[5]arene (**P10+**) was studied in solution with dynamic light scattering (DLS), methylene blue (MB) displacement assay, isothermal titration calorimetry (ITC), and anti-Xa-assay. With these methods, we verified that binding affinity towards heparin indeed increases with the increasing number of charges on the macrocycles.

However, the resorcin[4]arene with four protonated amines did not show any complexation with heparin under the physiologically relevant conditions and concentration ranges used in this study. As assumed, the anionic resorcinarene did not have any affinity towards heparin.

In addition to heparin binding, the host–guest system was able to detect heparin levels in application-relevant media. For this purpose, the most powerful host–guest combination is methyl orange (MO) as the guest, and **P10+** as the host in the 1 : 10 MO–**P10+** molar ratio. The detection is based on ratiometric sensing by monitoring the absorption maxima of free and bound MO. Moreover, a calibration curve for quantitative heparin dose detection in varying blood plasma contents was constructed.

## Results and discussion

Binding between the hosts and heparin was investigated through a series of DLS experiments. In these measurements, heparin solution was titrated with host solution and the hydrodynamic diameter and the count rate were monitored. As shown in Fig. 1a, **P10+** and protamine clearly display the increasing count rate up to the host-to-heparin mass ratio of 1.5 indicating heparin–host complex formation. Similar behavior was observed also for **R16+** and **R8+** only with lower count rates. Therefore, based on the count rate data, the optimal mass ratio for complex formation ranges between 1.25 and 1.5. In binding between **P10+** and heparin, these values correspond to a neutral charge balance, which is a well-known phenomenon in complex formation between oppositely charged polyelectrolytes.<sup>43,44</sup> In contrast, hosts **R16+** and **R8+** need a charge excess for full complexation of heparin. This difference might be due to better availability of binding sites in the bimodal structure of **P10+** when com-

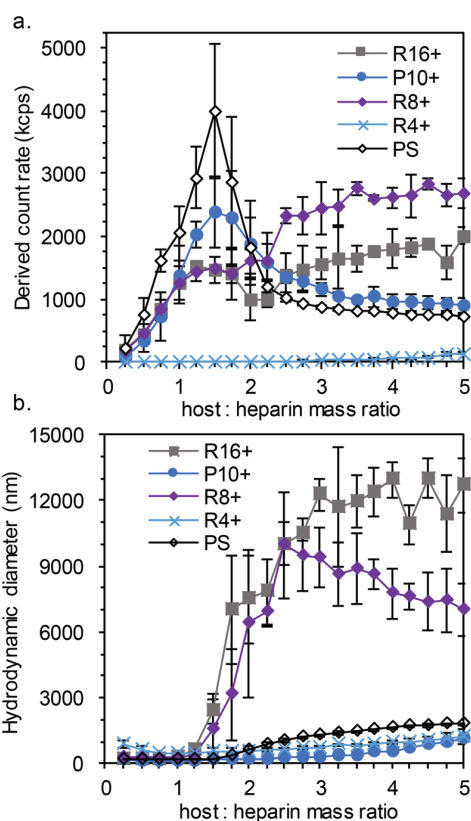


**Fig. 1** DLS data confirm complex formation between heparin and all the host molecules, except **R4+** and **R4-**, in physiologically relevant buffer (10 mM Tris-HCl, 150 mM NaCl, pH 7.4). (a) Count rate is highest at the host: heparin mass ratio 1.25–1.5 for **R16+**, **P10+**, **R8+** and protamine sulfate (PS). (b) Largest complexes are observed for **R16+** and **R8+** and smaller ones for **P10+** and protamine. Titrations were carried out in triplicates and averages with the standard deviation shown.

pared to the unimodal nature of the cationic groups in **R16+** and **R8+** (Scheme 1).

When the hydrodynamic diameter data are examined in detail, it is obvious that **R16+** and **R8+** form the largest complexes with heparin whereas **P10+** and protamine yield smaller host–heparin complexes (Fig. 1b). In previous studies, a structure- and concentration-dependent behavior of macrocycle–polyanion complexation has been observed. Therein, it was concluded that the long alkyl chains on the lower rim of the amphiphilic receptors induce the formation of smaller complexes of 50–60 nm.<sup>45,46</sup> However, our resorcin[4]arenes lack these long alkyl chains leading to the increase in complex sizes. In contrast, protamine and **P10+**, have no hydrophobic tails, meaning that only electrostatic interactions affect the binding process. For further confirmation of the complexation, all of these compounds (protamine, **R16+**, **P10+** and **R8+**) presented visually observable phase separation upon titration.

In both the count rate and the hydrodynamic diameter data, standard deviation values indicate that the complex size

and complex formation suffer from fluctuations. However, in signaling systems, a large complex size and the variation of the size are not destructive as long as they do not affect signaling accuracy.

Based on the DLS data of **R4+** and **R4-**, no complexation occurs between heparin and these resorcinarenes. For **R4+**, insignificant count rates and hydrodynamic diameters were measured but no confirmation of complex formation was detected even at high mass and charge ratios. This is most likely due to the low number of amine groups and steric hindrance caused by the cyclohexyl groups in the upper rim functionality. As expected, no presentable data of **R4-** were obtained as the measurements had too low count rates to produce reliable size data, making this receptor a good control compound. Additionally, neither of the titrations between heparin and hosts (**R4+** and **R4-**) resulted in any increase in the turbidity of the sample.

DLS studies of host molecule **P10+** were also carried out by including the guest molecule, methyl orange, into the system. In these measurements, no significant difference was observed when compared to the results without MO (Fig. S1†) indicating that host–guest binding does not interfere with the heparin–host complex formation.

From these measurements, it can be concluded that heparin binding is evident for hosts **R16+**, **P10+** and **R8+**, and it is as effective as for protamine. Additionally, binding is concentration- and structure-dependent, and is not affected by the host–guest complex formation.

The heparin neutralization efficiency of the host molecules was also studied with the methylene blue displacement assay in which the heparin–MB mixture was titrated with the host solution. Upon increasing the host concentration, the absorbance maximum shifts from 568 nm to 664 nm if methylene blue in the heparin–MB complex is released and replaced with the competing host. This kind of behavior was observed for host molecules **R16+**, **P10+** and **R8+** (Fig. 2), which is in good agreement with the DLS data. In particular, **R16+** and **P10+** have promising complexation profiles when compared to protamine, as they are almost equally efficient in heparin neutralization. Furthermore, based on Table 1, it seems that **P10+** is even more efficient than **R16+** as lower charge excess is needed with **P10+**. As was concluded also from the DLS data, this might be due to the better accessibility of the **P10+** charges as they are located on both sides of the molecules *versus* unimodal localization of the cationic groups on the resorcinarenes. Moreover, **R8+** shows complexation with heparin even though it is not as efficient as with **R16+**, **P10+** and protamine. As was observed also in the DLS measurements, **R4+** shows no complexation with heparin in the concentration ranges studied here. This can be attributed again to the lower number of charges when compared to the other hosts, steric hindrance caused by the cyclohexyl group in the **R4+** structure or due to lower binding affinity compared to MB. Additionally, as expected, negatively charged **R4-** does not show any complexation with the anionic heparin. Moreover, measurements with host **P10+** were also carried out together with the guest mole-

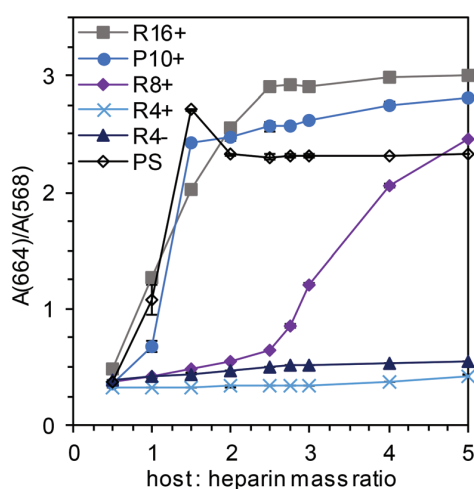


Fig. 2 Methylene blue displacement assay confirms concentration-dependent complex formation between heparin and hosts **R16+**, **P10+**, and **R8+** in 10 mM Tris-HCl, pH 7.4. Protamine (PS) is shown as a reference. Hosts **R4+** and **R4-** are not able to displace MB. The assay was performed three times and averages with the standard deviation shown.

**Table 1** Heparin and host binding parameters at a point of optimal binding based on DLS count rate data. Mass, molar and charge ratios (host:heparin) are presented. Charge ratios are calculated assuming that all primary, secondary and tertiary amines carry one positive charge and heparin with a molecular weight of 18 kDa has 90 charges<sup>47</sup>

Host	Mass ratio	Molar ratio	Charge ratio
<b>R16+</b>	1.25	11.07	1.97
<b>P10+</b>	1.5	11.89	1.32
<b>R8+</b>	1.5	22.87	2.03

cule, methyl orange. As in the DLS measurements, MO did not interfere with the host–heparin binding (Fig. S2†).

From these results, it can be concluded that **R16+** and **P10+** are the most promising alternatives for heparin binding and sensing. Overall, based on the differences observed here and in the previous studies on the electrostatic binding of heparin,<sup>16,18</sup> multivalency has high importance in the competitive heparin binding.

ITC measurements were conducted to further understand the thermodynamics of the host–heparin binding. The calorimetric titration plot obtained for **P10+** with heparin (Fig. 3 and Table S1†) indicates efficient binding between **P10+** and heparin and after background reduction results can be fitted with a sequential binding mode. The system corresponds roughly to binding saturation at a molar ratio of seven, which is in relatively good agreement with the 1:1 charge ratio observed also in the DLS data. The binding is enthalpy and entropy driven and spontaneous at 298 K. The first six binding interactions are very strong where the highest binding constant ( $K$ ) is  $2.75 \times 10^5 \text{ M}^{-1}$  and the lowest is  $6.39 \times 10^4 \text{ M}^{-1}$ . The last binding before saturation is relatively weak with a binding con-

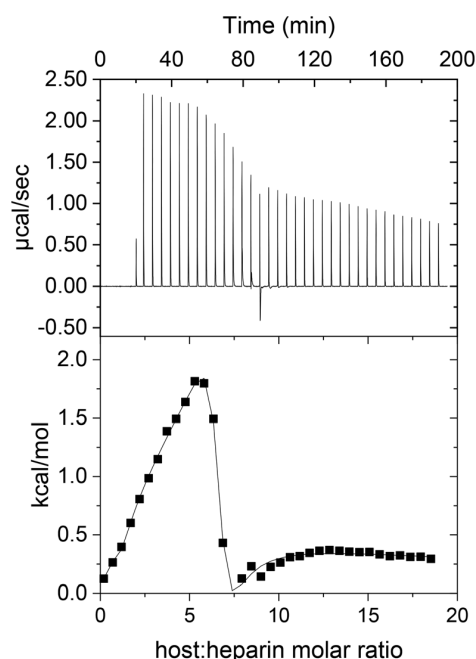
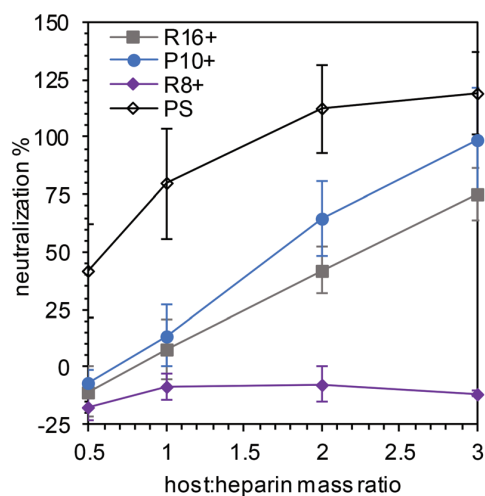


Fig. 3 ITC data of the titration of host **P10+** (5 mM) into heparin (0.05 mM) in 10 mM Tris-HCl buffer pH 7.4 at 298 K. The upper graph showing the raw data and the lower graph presenting the integrated data fitted into a sequential binding model after background reduction.

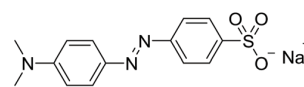
stant of  $1.29 \times 10^2 \text{ M}^{-1}$ . Additionally, binding between **R16+** and heparin follows the same trend but with less **R16+** molecules per heparin molecule as the stoichiometry is approximately six (Fig. S3a and Table S2†). All the binding sites indicate spontaneous binding and overall the binding is both entropy and enthalpy driven. The binding constants fluctuate but stay relatively strong between  $1.11 \times 10^3$  and  $6.31 \times 10^5 \text{ M}^{-1}$ . Furthermore, for **R8+**, the stoichiometry dropped to four molecules per heparin molecule and the spontaneous binding showed lower binding constants ( $1.25 \times 10^3$ – $1.95 \times 10^4 \text{ M}^{-1}$ ) compared to the other hosts (Fig. S3b and Table S3†). As with the other host molecules, **R8+** also showed both entropy and enthalpy driven interactions with heparin. Based on the results of the ITC measurements, we can further confirm the electrostatic binding between heparin and the host molecules also observed in the DLS and MB displacement assay experiments.

The *in vitro* heparin neutralization efficiency of the hosts was studied and compared to protamine by using a chromogenic 2-stage anti-Xa assay. In Fig. 4, it can be seen that neutralization effectiveness is dependent on the multivalency and concentration of the hosts. For instance, hosts **P10+** and **R16+** are relatively efficient in heparin neutralization, and increasing the host concentration enhances the neutralization up to 98% for **P10+**. In contrast, **R8+** does not show any efficiency in these concentrations, which is in line with the results from the MB displacement assay measurements. This lower binding

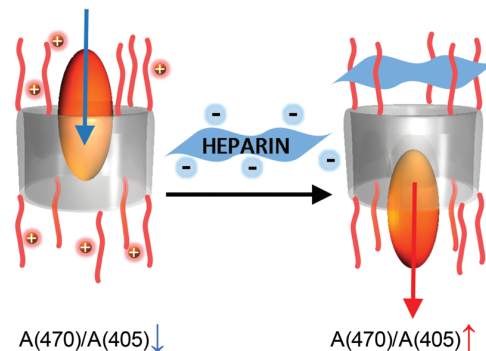


**Fig. 4** Anti-Xa assay performed in plasma proves that hosts **R16+** and **P10+** are effective heparin neutralizers in application-relevant media, and at high concentrations, they show activity comparable to the currently used heparin antidote, protamine sulfate (PS). In contrast, **R8+** is not effective in the concentration ranges used here. The assay was performed in triplicates and averages with the standard deviation shown.

**Guest: methyl orange (MO)**



**Host: P10+**



**Scheme 2** Structure of the guest methyl orange (MO), and schematic presentation of the host-guest binding between MO and **P10+** in addition to host-heparin binding.

efficiency even at high **R8+** concentrations is due to the lower number of charges that plays a key role especially in competitive media such as in blood plasma. Hosts **R4+** and **R4-** do not show any neutralization effect (Fig. S5†) as was concluded also from the DLS measurements and MB displacement assay experiments. A similar effect of the concentration and the number of charges on neutralization efficiency has also been detected previously with polymeric heparin binders.<sup>48–50</sup> In short, the anti-Xa assay confirms that heparin neutralization is efficient and linearly dose-dependent with hosts **P10+** and **R16+**. Moreover, at higher host concentrations, full neutralization of heparin is essentially achieved with **P10+**.

Host-guest binding between the cationic hosts and methyl orange was studied by using UV-Vis spectroscopy by comparing the absorption maxima corresponding to the free (470 nm) and bound (405 nm) states of MO (Scheme 2). In Fig. 5a, a clear decrease in the  $A(470)/A(405)$  ratio can be detected for host **P10+** indicating that it is the most effective receptor for MO. These data are derived from the original absorption spectra presented in Fig. 5b where a clear blue shift in the spectra is observed. Also hosts **R16+**, **R8+** and **R4+** are able to bind to the guest to some extent as can be concluded from the slight decrease of the  $A(470)/A(405)$  ratio as shown in Fig. 5a (original absorption spectra for all resorcin[4]arenes is presented in ESI Fig. S6†). However, the spectral changes are insignificant when compared to **P10+**. The decreased guest binding affinity of the resorcin[4]arene hosts is most probably due to their smaller cavity size and less complementary structure. Additionally, resorcinarenes used in this study exist in crown conformation due to the intramolecular hydrogen bonds of the upper rim hydroxyl groups thus leading to

shallow cavities. The tube-like cavity of the bimodal pillar[5]arene is larger and more complementary to the rod-like MO.<sup>51–54</sup> Protamine was used as a control and no changes in the MO spectra were observed indicating that protamine does not bind to MO (data not shown).

Host-guest binding between MO and hosts **R8+**, **P10+** and **R16+** was additionally investigated with ITC (Fig. S4†) at 298 K. The binding between host **P10+** and MO was further confirmed from this ITC analysis, which reveals the complexation to be exothermic, enthalpy driven and spontaneous ( $\Delta H < 0$ ,  $T\Delta S < 0$ ,  $\Delta G < 0$ ). Moreover, binding is relatively strong with a binding constant of  $1.02 \times 10^5 \pm 0.211 \text{ M}^{-1}$  in 1:1 binding mode. In comparison, the ITC data of **R8+** and **R16+** with MO show the binding to be unspecific clearly suggesting a very weak or no binding process. In addition, NMR studies were conducted to monitor the host-guest binding between host **P10+** and guest MO. As shown in Fig. 5c, the <sup>1</sup>H NMR spectra show clear upfield shifts of aromatic signals of MO as a result of shielding, thus clearly confirming the inclusion complex between **P10+** and MO. Host-guest binding between cationic pillararenes and MO has also been studied before in water.<sup>55</sup> The results presented here confirm binding between pillar[5]arene and MO in physiologically relevant media even though the protonation stage of MO has been shown to have an influence on the binding mode.<sup>56</sup> In the previously published study, the inclusion complex is suggested to form in such a manner that the hydrophobic part of MO is inside the cavity and the sulfonated anionic head is outside the cavity. Based on the DLS and MB displacement assay studies performed in this work, no negative effect of this kind of host-guest binding on host-heparin binding was identified. In conclusion, based

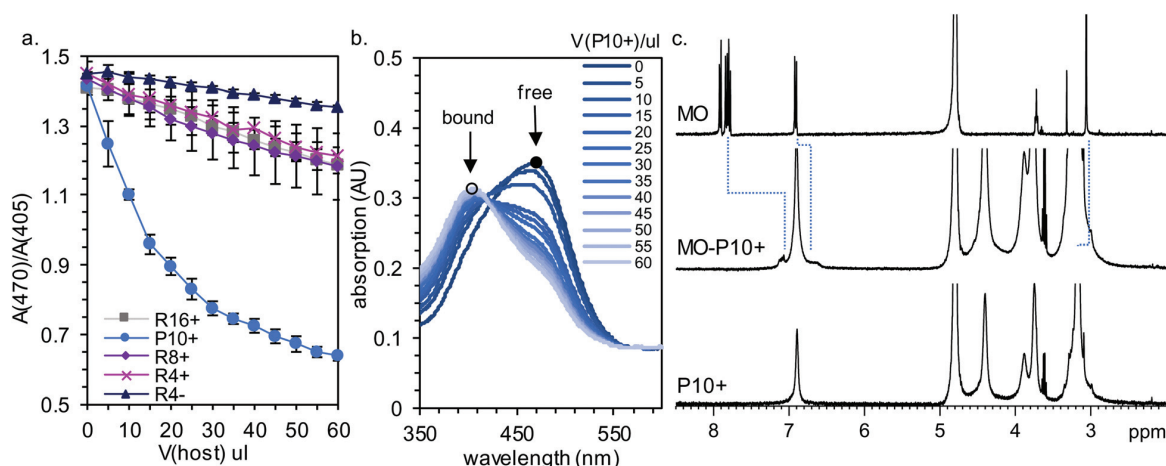


**Fig. 5** Complexation between the hosts and the guest (MO) was studied by using UV-Vis spectroscopy in physiologically relevant Tris-HCl buffer (10 mM Tris 150 mM NaCl, pH 7.4). (a) By comparing the absorption maxima of free (470 nm) and bound (405 nm) methyl orange, host-guest complex formation can be monitored. Inclusion of MO is most pronounced with host **P10+**. Titrations were carried out in triplicates and averages with the standard deviation are presented. (b) A blue shift in the absorption spectra is observed when MO solution is titrated with host **P10+**. (c) Host-guest binding was confirmed by  $^1\text{H}$  NMR spectroscopy where a clear shift of the aromatic signals of the guest is observed confirming the formation of the inclusion complex.

on the superior host-guest binding results obtained with **P10+**, further application-relevant studies were continued with only host **P10+**.

In the next step, heparin's effect on the host-guest binding and especially absorption properties of methyl orange was studied. In general, the titration of MO-P10+ solution with

heparin leads to the increase in the  $A(470)/A(405)$  ratio (Fig. 6) indicating that the interaction with heparin releases the MO from the host cavity. Analogous MO displacement behavior has also been observed before for a similar triplicate system consisting of cationic resorcinarenes, methyl orange and polyacrylic acid.<sup>51</sup> However, in the system presented here, the

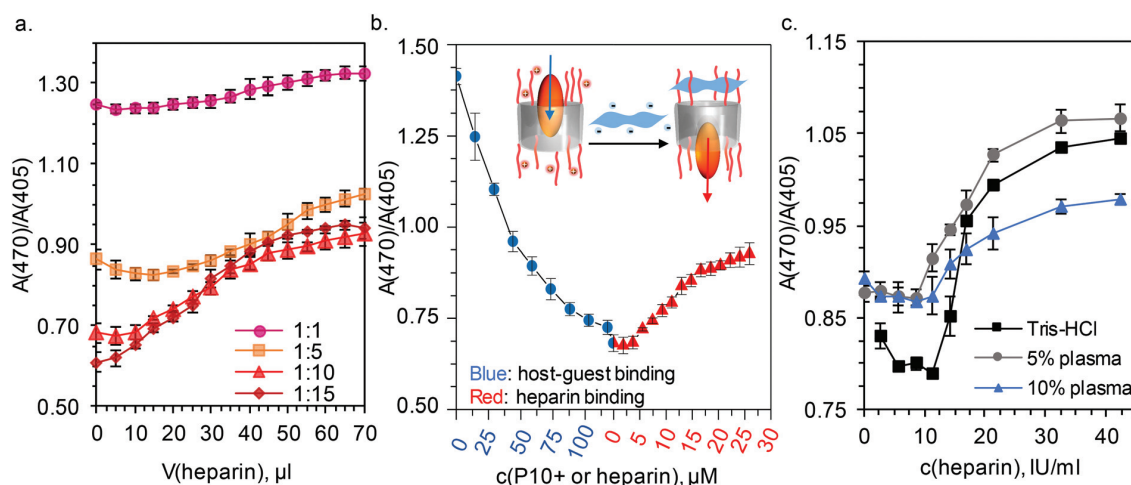


**Fig. 6** Host-guest complexes of methyl orange ( $0.06 \text{ mg ml}^{-1}$ ) and **P10+** ( $0.42\text{--}6.24 \text{ mg ml}^{-1}$ ) with different molar ratios (1 : 1, 1 : 5, 1 : 10 and 1 : 15) were titrated with heparin to find the most optimal mixture for monitoring heparin levels. Release of MO upon heparin addition was observed by UV-Vis spectroscopy and by comparing the absorption maxima of free (470 nm) and bound (405 nm) MO. (b) By combining the data from host-guest titration and heparin titration, it was observed that around 40% of the MO (from the  $A(470)/A(405)$  ratio) is recovered upon heparin additions. Blue spheres: MO titrated with host **P10+**, red triangles: MO-P10+ titrated with heparin. (c) Calibration curves for different plasma concentrations were formed by adding MO-P10+ solution (1 : 10 MO-P10+ molar ratio,  $4.1 \text{ mg ml}^{-1}$  **P10+** and  $0.06 \text{ mg ml}^{-1}$  MO) to heparinized samples. Data were recorded after 10 minute stabilization time. The clearest increase in the  $A(470)/A(405)$  ratio is observed for Tris-HCl without plasma but 5% plasma content yields the smoothest linearity over the largest heparin concentration range. All titrations were carried out in triplicates and averages with the standard deviation are presented.

host-guest binding likely has more specificity as the pillararene cavity is more confined. In order to optimize our system, heparin titrations were carried out with varying host-guest molar ratios to obtain the ideal combination for heparin concentration monitoring. From the experiments, it was observed that the 1:10 molar ratio of the host to guest is ideal as a clear plateau is observed (Fig. 6a) unlike with the 1:5 ratio, and moreover, the further increase of the guest concentration to the molar ratio of 1:15 did not improve the recovery of the  $A(470)/A(405)$  ratio. The original absorption spectra of all molar ratios are presented in the ESI (Fig. S7†). From the  $A(470)/A(405)$  ratio, it is clear that the addition of heparin to the host-guest mixture did not fully release the MO from the host cavity (Fig. 6b). However, correlation between the heparin concentration and the  $A(470)/A(405)$  ratio is linear with only minor standard deviations, which is crucial for the signaling system. Highlighting the profitability of our host-guest binding system, the amounts of the host and guest are reasonable in contrast to a previously published study,<sup>16</sup> based on calix[8]arenes and fluorescent eosin-Y, where nearly 1000 times higher molar ratio of calixarene : eosin-Y was needed for clear signaling.

In general, the host-guest complex needs to be selective towards heparin in order to perform properly in the application-relevant media consisting of competing compounds. Therefore, the selectivity of host **P10+** towards heparin was studied by comparing it with other glycosaminoglycans. As expected and based on the high negative charge of heparin, **P10+** is most selective towards heparin, as hyaluronic acid and chondroitin sulfate show nearly no competition with heparin (Fig. S8†). The analogous selectivity profile has also been observed in other previously reported colorimetric<sup>11</sup> and fluorescent<sup>32</sup> sensing systems designed for heparin.

Moreover, it was shown that with this system, a calibration curve for quantitative measurements can be successfully produced, and additionally, the effect of increasing the plasma content can be evaluated. Buffer solutions with varying plasma contents were heparinized with 2.8–42.4 IU ml<sup>-1</sup> heparin concentration. To these heparinized samples, 30 µl of MO-**P10+** solution with the 1:10 molar ratio (4.1 mg ml<sup>-1</sup> **P10+** and 0.06 mg ml<sup>-1</sup> MO concentration) was added. Absorption spectra stabilized quickly after MO-**P10+** addition (Fig. S9†), and therefore, 10 minutes was chosen as the stabilization time for conducting the calibration curve. From Fig. 6c, it can be observed that in Tris-HCl buffer without plasma, variances between different heparin concentrations are the clearest, but the linear region is slightly reduced when compared to 5% plasma samples, which show a linear dependence between the heparin concentration and the  $A(470)/A(405)$  ratio with heparin concentrations ranging from 8.5 to 21.2 IU ml<sup>-1</sup>. For both sample sets, before the linearly increasing region, no response is observed, and after the linear region, a plateau is gradually reached. Samples with 10% plasma suffer from insignificant differences between different heparin concentrations and from the most prominent standard deviations. Similar disruption by increasing the plasma concentration in heparin binding has

previously been detected in other heparin sensing systems.<sup>18</sup> From the minor standard deviations in 0 and 5% plasma samples, it can be concluded that large deviations observed in the DLS data do not prevent accurate sensing. To improve the system, for example, binding affinity between heparin and the host could be enhanced, as the system should also be operational at lower application-relevant heparin concentrations (2–8 IU mL<sup>-1</sup> (17–67 µM) during cardiovascular surgery and 0.2–1.2 IU mL<sup>-1</sup> (1.7–10 µM) in postoperative and long-term care).<sup>57</sup> The increased heparin binding affinity could, for instance, be achieved by further enhancing the multivalency or by increasing the sensor concentration.<sup>18</sup> Binding affinity can also be enhanced by increasing the binding surface allowing more simultaneous interactions with heparin.<sup>15</sup> On the other hand, by lowering the host-guest binding affinity, which is based on the fact that ITC measurement is high, one could more easily release the guest from the host cavity upon heparin binding.

## Conclusions

In summary, we have shown that macrocyclic hosts are efficient heparin binders, and by introducing a guest molecule to the system, they can also be simultaneously utilized in heparin concentration monitoring. In the heparin neutralization studies, it was observed that multivalency plays a key role when macrocyclic host molecules are used in the electrostatic binding of heparin. Based on DLS, methylene blue displacement assay, ITC and anti-Xa studies, binding was efficient in competitive, application-relevant media with both pillar[5]arene and resorcin[4]arenes when the molecules had a sufficient number of positive charges. Interestingly, host **P10+** was the best performing host and essentially, it was capable of full heparin neutralization. Additionally, the host-guest complexation does not interfere with the host-heparin binding making the host-guest complex of **P10+** and methyl orange an effective heparin binder and sensor. Ratiometric data for heparin concentration monitoring are obtained by comparing the bound and free absorption maxima of the guest, MO. Furthermore, based on this approach, a calibration curve for the quantitative detection of heparin levels in varying amounts of plasma was conducted. We suggest that by further enhancing the sensing abilities at low heparin levels, the host-guest complexes are promising heparin binders and sensors. In conclusion, this study gives a deeper understanding of the possibilities of macrocyclic receptors in a signaling system. We envision that based on the thorough solution state measurements, other tertiary supramolecular host-guest-polymer systems can be developed, for example, for biomedical applications.

## Conflicts of interest

There are no conflicts to declare.

## Acknowledgements

The authors gratefully acknowledge financial support from the Academy of Finland (grant no. 263504, 267497, 273645, 286845 and 308578), Aalto University School of Chemical Engineering, Jane and Aatos Erkko Foundation, Biocentrum Helsinki and the University of Windsor, ON, Canada. This work was carried out under the Academy of Finland's Centres of Excellence Programme (HYBER 2014–2019). The authors wish to thank Lotta Gustavsson for assisting in the UV-Vis measurements.

## References

- B. Casu, A. Naggi and G. Torri, *Carbohydr. Res.*, 2015, **403**, 60–68.
- J. Hirsh, T. E. Warkentin, S. G. Shaughnessy, S. S. Anand, J. L. Halperin, R. Raschke, C. Granger, E. M. Ohman and J. E. Dalen, *Chest*, 2001, **119**, 64S–94S.
- S. M. Bromfield, E. Wilde and D. K. Smith, *Chem. Soc. Rev.*, 2013, **42**, 9184–9195.
- R. Balhorn, *Genome Biol.*, 2007, **8**, 227.
- J. C. Horrow, *Anesth. Analg.*, 1985, **64**, 348–361.
- S. Wan, J.-L. LeClerc and J.-L. Vincent, *Chest*, 1997, **112**, 676–692.
- M. Nybo and J. S. Madsen, *Basic Clin. Pharmacol. Toxicol.*, 2008, **103**, 192–196.
- J. W. Vandiver and T. G. Vondracek, *Pharmacotherapy*, 2012, **32**, 546–558.
- S. Kitchen, *Br. J. Haematol.*, 2000, **111**, 397–406.
- M. D. Klein, R. A. Drongowski, R. J. Linhardt and R. S. Langer, *Anal. Biochem.*, 1982, **124**, 59–64.
- Z. Zhong and E. V. Anslyn, *J. Am. Chem. Soc.*, 2002, **124**, 9014–9015.
- K.-Y. Pu and B. Liu, *Macromolecules*, 2008, **41**, 6636–6640.
- T. Bříza, Z. Kejík, I. Císařová, J. Králová, P. Martásek and V. Král, *Chem. Commun.*, 2008, 1901–1903.
- S. M. Bromfield, A. Barnard, P. Posocco, M. Fermeglia, S. Priel and D. K. Smith, *J. Am. Chem. Soc.*, 2013, **135**, 2911–2914.
- A. T. Wright, Z. Zhong and E. V. Anslyn, *Angew. Chem., Int. Ed.*, 2005, **44**, 5679–5682.
- T. Mecca, G. M. L. Consoli, C. Geraci, R. L. Spina and F. Cunsolo, *Org. Biomol. Chem.*, 2006, **4**, 3763–3768.
- Y. Egawa, R. Hayashida, T. Seki and J. Anzai, *Talanta*, 2008, **76**, 736–741.
- C. W. Chan and D. K. Smith, *Chem. Commun.*, 2016, **52**, 3785–3788.
- M. Wang, D. Zhang, G. Zhang and D. Zhu, *Chem. Commun.*, 2008, 4469–4471.
- S. Wang and Y.-T. Chang, *Chem. Commun.*, 2008, 1173–1175.
- L. Zeng, P. Wang, H. Zhang, X. Zhuang, Q. Dai and W. Liu, *Org. Lett.*, 2009, **11**, 4294–4297.
- Y. Ling, Z. F. Gao, Q. Zhou, N. B. Li and H. Q. Luo, *Anal. Chem.*, 2015, **87**, 1575–1581.
- M. Yang, J. Chen, H. Zhou, W. Li, Y. Wang, J. Li, C. Zhang, C. Zhou and C. Yu, *Biosens. Bioelectron.*, 2016, **75**, 404–410.
- R. B. C. Jagt, R. F. Gómez-Biagi and M. Nitz, *Angew. Chem., Int. Ed.*, 2009, **48**, 1995–1997.
- H. Szelke, S. Schübel, J. Harenberg and R. Krämer, *Chem. Commun.*, 2010, **46**, 1667–1669.
- M. C.-L. Yeung and V. W.-W. Yam, *Chem. – Eur. J.*, 2011, **17**, 11987–11990.
- Q. Chen, Y. Cui, J. Cao and B.-H. Han, *Polymer*, 2011, **52**, 383–390.
- K.-Y. Pu and B. Liu, *Adv. Funct. Mater.*, 2009, **19**, 277–284.
- W. Sun, H. Bandmann and T. Schrader, *Chem. – Eur. J.*, 2007, **13**, 7701–7707.
- L.-J. Chen, Y.-Y. Ren, N.-W. Wu, B. Sun, J.-Q. Ma, L. Zhang, H. Tan, M. Liu, X. Li and H.-B. Yang, *J. Am. Chem. Soc.*, 2015, **137**, 11725–11735.
- J. C. Saucedo, R. M. Duke and M. Nitz, *ChemBioChem*, 2007, **8**, 391–394.
- Y. Ding, L. Shi and H. Wei, *Chem. Sci.*, 2015, **6**, 6361–6366.
- P. Timmerman, W. Verboom and D. N. Reinhoudt, *Tetrahedron*, 1996, **52**, 2663–2704.
- K. Yang, Y. Pei, J. Wen and Z. Pei, *Chem. Commun.*, 2016, **52**, 9316–9326.
- X. Ma and Y. Zhao, *Chem. Rev.*, 2015, **115**, 7794–7839.
- C. B. Rodell, J. E. Mealy and J. A. Burdick, *Bioconjugate Chem.*, 2015, **26**, 2279–2289.
- F. Pan, N. K. Beyeh and K. Rissanen, *J. Am. Chem. Soc.*, 2015, **137**, 10406–10413.
- W. Iwanek and J. Mattay, *Liebigs Ann.*, 1995, **1995**, 1463–1466.
- N. K. Beyeh, H. H. Jo, I. Kolesnichenko, F. Pan, E. Kalenius, E. V. Anslyn, R. H. A. Ras and K. Rissanen, *J. Org. Chem.*, 2017, **82**, 5198–5203.
- N. K. Beyeh, I. Díez, S. M. Taimoory, D. Meister, A. I. Feig, J. F. Trant, R. H. A. Ras and K. Rissanen, *Chem. Sci.*, 2018, **9**, 1358–1367.
- V. Montes-García, C. Fernández-López, B. Gómez, I. Pérez-Juste, L. García-Río, L. M. Liz-Marzán, J. Pérez-Juste and I. Pastoriza-Santos, *Chem. – Eur. J.*, 2014, **20**, 8404–8409.
- K. Kobayashi, Y. Asakawa, Y. Kato and Y. Aoyama, *J. Am. Chem. Soc.*, 1992, **114**, 10307–10313.
- A. S. Michaels, *Ind. Eng. Chem.*, 1965, **57**, 32–40.
- J. van der Gucht, E. Spruijt, M. Lemmers and M. A. Cohen Stuart, *J. Colloid Interface Sci.*, 2011, **361**, 407–422.
- V. Bagnacani, V. Franceschi, M. Bassi, M. Lomazzi, G. Donofrio, F. Sansone, A. Casnati and R. Ungaro, *Nat. Commun.*, 2013, **4**, 1721.
- R. V. Rodik, A. S. Klymchenko, N. Jain, S. I. Miroshnichenko, L. Richert, V. I. Kalchenko and Y. Mély, *Chem. – Eur. J.*, 2011, **17**, 5526–5538.
- I. Capila and R. J. Linhardt, *Angew. Chem., Int. Ed.*, 2002, **41**, 390–412.
- S. Välimäki, A. Khakalo, A. Ora, L.-S. Johansson, O. J. Rojas and M. A. Kostianen, *Biomacromolecules*, 2016, **17**, 2891–2900.

- 49 R. A. Shenoi, M. T. Kalathottukaren, R. J. Travers, B. F. L. Lai, A. L. Creagh, D. Lange, K. Yu, M. Weinhart, B. H. Chew, C. Du, D. E. Brooks, C. J. Carter, J. H. Morrissey, C. A. Haynes and J. N. Kizhakkedathu, *Sci. Transl. Med.*, 2014, **6**, 260ra150.
- 50 M. T. Kalathottukaren, S. Abbina, K. Yu, R. A. Shenoi, A. L. Creagh, C. Haynes and J. N. Kizhakkedathu, *Biomacromolecules*, 2017, **18**, 3343–3358.
- 51 J. E. Morozova, V. V. Syakaev, A. M. Ermakova, Y. V. Shalaeva, E. K. Kazakova and A. I. Konovalov, *Colloids Surf., A*, 2015, **481**, 400–406.
- 52 T. Ogoshi, H. Kayama, D. Yamafuji, T. Aoki and T. Yamagishi, *Chem. Sci.*, 2012, **3**, 3221–3226.
- 53 B. Hua, L. Shao, Z. Zhang, J. Sun and J. Yang, *Sens. Actuators, B*, 2018, **255**, 1430–1435.
- 54 G. Yu, J. Zhou, J. Shen, G. Tang and F. Huang, *Chem. Sci.*, 2016, **7**, 4073–4078.
- 55 L. S. Yakimova, D. N. Shurpik, L. H. Gilmanova, A. R. Makhmutova, A. Rakhimbekova and I. I. Stoikov, *Org. Biomol. Chem.*, 2016, **14**, 4233–4238.
- 56 S. He, X. Sun and H. Zhang, *J. Mol. Struct.*, 2016, **1107**, 182–188.
- 57 J. Hirsh and R. Raschke, *Chest*, 2004, **126**, 188S–203S.